U. D. C. 541.14 : 541.13

The Photoelectric Effect at the Metal-Electrolyte Boundary

L.I.Korshunov, Ya.M.Zolotovitskii, and V.A.Benderskii

Photoelectrochemistry is a new branch of physical chemistry, with many applications in the study of boundary layer structure, the energetics of electrons in solutions, the mechanism of photoemission, and the kinetics of fast reactions in solutions initiated by solvated electrons. 110 references.

CONTENTS

I.	Introduction	699
II.	Experimental methods	699
III.	General aspects of photoemission into electrolyte solutions and ionisation of surface donor-acceptor complexes	701
IV.	Status of the "five-over-two" law and of the distribution function of solvated electrons	705
V.	Tunnelling of emitted electrons through the potential barrier at the interface	706
VI.	Photoemission from metals into electrolyte solutions as a method of studying fast reactions	707
VII.	Work function of electrons from metals into polar solvents	709
VIII.	Multi-photon photoemission from mercury into electrolyte solutions and pulse heating of the solution	710
IX.	Charge transfer through the electrode-solution interface during photochemical reactions in solutions	711

I. INTRODUCTION

The generation of photocurrents by illumination of the interface between an electrode and an electrolyte solution was first reported by Becquerel over 100 years ago[1]. However, the elementary acts involved in the electrode photoeffect have only recently been characterised by work done at Harwell (England)[2-4] and at the Chemical Physics and the Electrochemistry Institutes of the USSR Academy of Sciences[5-11].

According to current views, the following charge separation processes have to be considered when a metal-solution interface is illuminated: 1) photoemission of electrons from the metal into the electrolyte solution; 2) photoionisation of the surface donor-acceptor complexes which include the electrode as one component; 3) electrode reactions involving metastable species produced by the interaction of photoemitted electrons with the molecules of the medium; 4) electrode reactions involving the products of photochemical reactions in solution.

In real systems these processes usually overlap, and complicated experimental procedures are needed to resolve them.

This review is concerned with elementary, light-induced charge transfer processes at the metal-electrolyte boundary: a) in solutions which do not absorb in the spectral region used to excite the electrode, and b) in solutions of photochemically active redox systems, including a light-absorbing dye.

The electrode photoeffect has great theoretical and practical interest. Photo-emission from metals into electrolyte solutions offers a new approach to the study of the behaviour of low-energy electrons in condensed media. Its characteristics are directly determined by the structure of the interfacial boundary layer and by the physicochemical properties of the solution.

The photoelectrochemical method of detecting unstable species in solution is much more sensitive than alternative methods such as optical and radiation methods.

II. EXPERIMENTAL METHODS

The electrode photoeffect can be studied by three methods: with constant illumination, interrupted illumination, and pulse illumination. The relaxation methods are by far the more important, because they give both the magnitude and the kinetic constants of the photoeffect.

The photocurrent in an electrochemical cell exposed to steady light can be measured with a sensitive galvanometer[11] or a polarograph[13]. The success of the method depends on the purity of the reagents, since it is essential to avoid significant Faradaic currents in this work. Intermittent photocurrent is obtained by modulating the light supplied to the electrode. Barker[3] used a square-wave polarograph to measure intermittent photocurrents (f = 225 Hz). For sinusoidal modulation, the measuring equipment consists of a narrow-band amplifier tuned to the modulation frequency, followed by a synchronous detector[10]. The current-voltage curve for the photoeffect is plotted directly, by sweeping the voltage (Figs. 1 and 2). An apparatus has been described[14] in which the impedance of an electrochemical cell can be measured by sinusoidally modulating the illumination or by applying a small alternating voltage. The measurements of the components of the photoimpedance, proposed by Rotenberg and coworkers[15], has not yet been realised experimentally.

The pulse method was first applied by Berg[16]. One form[8] of the apparatus is shown in Fig. 3. The photopotential which appears across a standard resistor in series with the cell is displayed on a double-beam oscilloscope. The second channel of the oscilloscope is used to record the wave-form of the light pulse (Fig. 4).

Powerful light pulses in the visible and the ultraviolet region of the spectrum are obtained by means of mercury or xenon lamps. Lasers also are a convenient source of radiation[9,17].

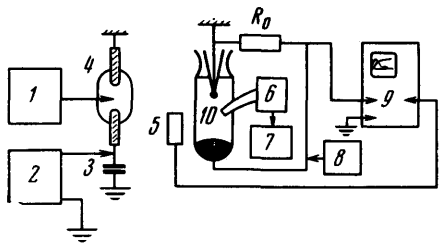


Figure 1. Pulse apparatus: *1*) firing circuit; *2*) condenser charging circuit; *3*) pulse condenser; *4*) flash lamp; *5*) synchronising photodiode; *6*) reference electrode; *7*) potentiometer for the working electrode; *8*) commutator circuit for measuring the capacity of the working electrode; *9*) oscilloscope; *10*) polarographic cell; R_0 is the standard resistor.

An analysis of the equivalent circuit of the cell shows that the measured signal $V_{ph}(t)$ is related to the photocurrent $I_{ph}(t)$ flowing through the interface by the expression

$$V_{ph}(t) = \exp(-t/RC) \int_0^t 1/C I_{ph}(t') \exp(t'/RC)\, dt' \qquad (1)$$

where t is time, R is the resistance of the circuit, and C is the capacity of the electrical double layer (~16 μF cm^{-2}).

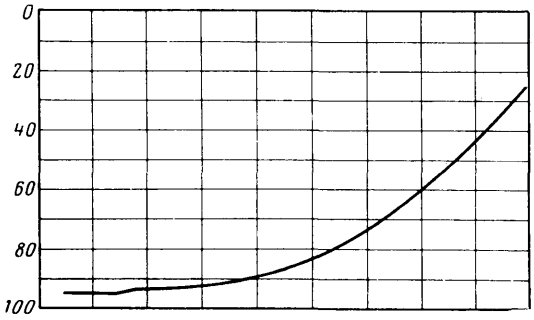


Figure 2. Plot of the photocurrent obtained by sweeping the potential. The potential is plotted horizontally and the photocurrent vertically.

For pulse measurements the standard resistance is chosen to give an RC value much greater than the duration of the pulse of photocurrent. In this case, $V_{ph}(t) = \int_0^t C^{-1} \cdot I_{ph}(t')dt'$, i.e. the measured photopotential is proportional to the charge transferred across the interface. With the dropping mercury electrode—a very convenient photocathode—the condition is satisfied by taking $R \geqslant 10^5$ ohm for pulse durations of 10^{-5}–10^{-3} s. The capacity, which must be known in order to calculate the charge, is measured by the commutator method[18].

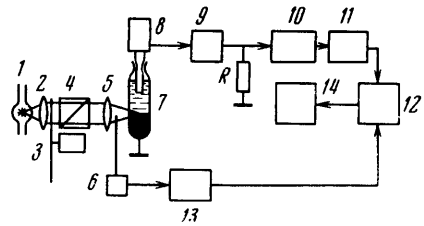


Figure 3. Apparatus for intermittent illumination: *1*) DRSh-1000 lamp; *2*) quartz lens; *3*) chopper; *4*) Glan Nicol prism; *5*) quartz condenser; *6*) photodiode; *7*) photocathode; *8*) polarisable reference electrode; *9*) polarising circuit; *10*), *11*), *13*) V6-2 amplifiers; *12*) KZ-2 synchronous detector; *14*) chart recorder.

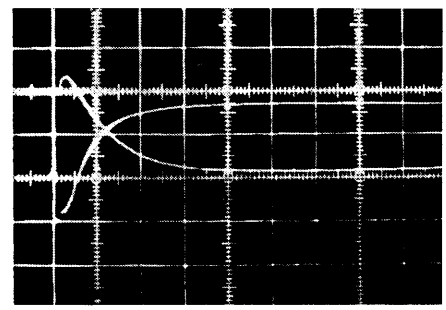


Figure 4. Oscillograms of the photoemission signal $V(t)$ (upper trace) and of the light pulse $L(t)$ (lower trace). Calibration: 200 μs cm^{-1} (horizontal axis) and 1 mV cm^{-1} (vertical axis).

In Delahay's differential method[19], the potential difference between two identical electrodes (one of which is kept in the dark while the other is exposed to a pulse of light) is measured. With modulated or steady illumination one usually measures the quantity $V_{ph}(t) = I_{ph}(t) \cdot R$. This regime corresponds to the condition $\omega_M RC \ll 1$, where ω_M is the modulation frequency. For a dropping electrode this condition is satisfied by $R \leqslant$ 500 ohm and $\omega_M \leqslant 10^3$ Hz. An analysis of the measurement errors[20] has shown that in the steady illumination regime the error is usually 3–4%, as compared with 7–8% for pulses of 10^{-6}–10^{-7} s duration. The precision of the pulse method can be increased by using storage oscilloscopes and amplitude–time analysers for the microsecond range[21]. Stroboscopic light sources, including

pulsed gas lasers, are very important in studies of the relaxation phenomena associated with photoemission. They are used in conjunction with signal averaging devices [22].

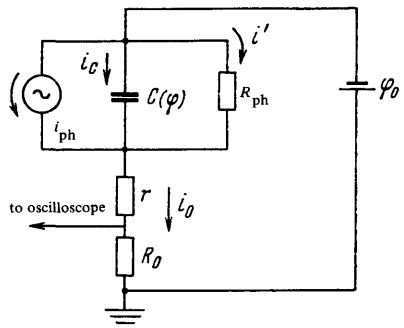


Figure 5. Equivalent circuit of the electrochemical cell during the passage of photocurrent.

Korshunov and coworkers [22] illuminated the electrode–solution interface with pulses from a nitrogen laser ($\lambda = 3371$ Å) of 20 ns duration at the 0.35 level. The time resolution of the apparatus was 10 ns. In order to avoid the slow ($10^{-7}-10^{-5}$ s) signal fluctuations due to electrocapillary effects, the dropping mercury electrode was replaced by an amalgamated gold wire ($s = 2.5 \times 10^{-3}$ cm^2). In order to match the signal to the input of the measuring apparatus, a standard resistance of 150 ohm was used. The time constant of the integrating circuit ($\sim 2 \times 10^{-5}$ s) allowed processes occurring over periods of $10^{-8}-10^{-5}$ s to be studied. The repetition frequency of the laser pulses was 50 Hz.

III. GENERAL ASPECTS OF PHOTOEMISSION INTO ELECTROLYTE SOLUTIONS AND IONISATION OF SURFACE DONOR–ACCEPTOR COMPLEXES

The concepts of cathodic photocurrent due to u.v. illumination of solutions of indifferent electrolytes, and of the emission of electrons from an electrode into a solution, are both due to Barker [2]. Earlier, pioneering work on the electrode photoeffect includes Heyrovsky's hypothesis [23-27] of the surface donor–acceptor complex and Berg's "hot electrode" concept [28-33]. Heyrovsky considered that the photocurrent is produced by ionisation of a surface donor–acceptor complex, consisting of the electrode on the one hand and the solvent or solute on the other hand. Absorption of a light quantum raises the complex to an excited state. The direction of the electron transfer (i.e. the sign of the photocurrent) depends on the relative positions of the energy levels of the complex, the energy level of the electrode being determined by the electrode potential φ. Heyrovsky's hypothesis was based on the observation of anodic photocurrents at $\varphi > \varphi_{z.c.}$, where $\varphi_{z.c.}$ is the potential at the point of zero charge, in solutions of organic molecules containing the functional group $-\underset{\underset{O}{\|}}{C}-\underset{\underset{X}{|}}{C}=$.

The formation of surface donor–acceptor complexes has since been confirmed for a number of compounds, but only at $\varphi > \varphi_{z.c.}$ [10].

According to Berg, the photoexcitation of electrons in the metal causes the electrolyte ions to be discharged at more positive potentials. The suggestion had been put forward earlier by Bowden [34], who had observed a decrease of hydrogen overvoltage at an illuminated electrode. However, since the relaxation time of the charge in the metal [35] is less than 10^{-16} s, this mechanism cannot be accepted.

Barker based his hypothesis on a detailed study of the spectral and current–voltage characteristics of the electrode photoeffect, because properties such as proportionality to the light intensity, short persistence, and the presence of a long-wave threshold can be explained by almost any model. We shall discuss the problem in some detail in the following paragraphs.

Photoemission from metals into electrolyte solutions can be treated as three distinct steps: a) interaction of a photon with the conduction electrons of the metal, causing an electron to pass through the potential barrier at the interface; b) thermalisation and solvation of the emitted electron in the solution medium; c) chemical and electrode reactions of the solvated electron, and of the products of its interaction with acceptor molecules present in solution.

The first step in photoemission is quite different from photoemission into a vacuum, because of the sharp drop in potential across the electrical double layer over distances of 10 Å or less (in concentrated solutions), and because of the Coulombic screening of the emitted electron with respect to the image forces.

The double layer at the interface affects the emission properties of the metal electrode, because the emitted electrons can tunnel through the dense part of the double layer, thus lowering the work function of the metal by an amount equal to the applied potential. The screening effect operates on the positive charge in the metal electrode produced by the emission of an electron, and is due to the ions in the electrical double layer. (The electron in the solution is screened much more slowly). According to Brodskii and Gurevich [6], this effect should result in the replacement of Fowler's parabolic law [36,37] by a "five-over-two" law of the form

$$I_0 = L\chi(\omega)(h\omega - h\omega_0 - e\varphi)^{5/2} \qquad (2)$$

where L is the light intensity, $\chi(\omega)$ is a function of the properties of the metal and of conditions of light absorption, h is Planck's constant, ω is the frequency of the incident light, ω_0 is the frequency of the long-wave limit of the photoeffect, e is the electronic charge, and φ is the potential of the electrode relative to the potential at the point of zero charge.

The second step in photoemission is the least well understood at the moment, because very little is known about the differential scattering cross-sections of low-energy electrons (0.5–3 eV) in condensed media. If we assume that the main scattering mechanism in water is dipole relaxation, the characteristic thermalisation time works out [38] to $10^{-12}-10^{-13}$ s. The time for the hydration of an electron, i.e. the time needed to convert it into a polaron state, is [38] $\sim 10^{-12}$ s.

The third step in photoemission concerns the behaviour of the electrons after thermalisation and hydration. Such electrons can be captured by acceptors in solution, or they can return to the electrode. The capture of a solvated electron by an acceptor is diffusion-controlled,

with a characteristic time of $10^{-6}-10^{-9}$ s depending on the concentration of the acceptor. The molecule containing a trapped electron can itself undergo homogeneous or heterogeneous (electrode) reactions; furthermore, the homogeneous reaction product can undergo further reaction at the electrode. Thus, the experimentally observed photocurrent depends, in general, on the emission current I_0, the diffusion current of electrons returning from the solution I_1, and the currents (I_{2i}) due to the electrode reactions of the species produced from the acceptor containing a trapped electron:

$$I = I_0 - I_1 + \sum_i I_{2i}$$

Various electron acceptors are added to the solution in order to minimise the reverse diffusion current I_1: these can be neutral (N_2O, CO, acrylonitrile), positively charged (H^+), or negatively charged (NO_3^-, NO_2^-, BrO_3^-, CN^-, SeO_3^-, TeO_4^-, etc.) [2,27].

Barker solved the steady-state problem for the simplest case (no side reactions) by the equivalent circuit method[3]. Sinusoidally modulated[39] and pulsed[20] illumination were treated separately. Solution of the non-stationary diffusion equation gives the following expression for the photocurrent produced by illumination for times longer than the times involved in the reverse current of solvated electrons and in electron capture by the acceptors (estimated to be less than 10^{-6} s):

$$I = L(t)\int_0^\infty f(x)\left\{1-\exp\left(-\sqrt{\frac{kc}{D_s}}\,x\right)\right\}dx \qquad (3)$$

Under these conditions, $I_0 = L(t)\int_0^\infty f(x)dx$, where $L(t)$ is the intensity of the exciting light, $f(x)$ is a function of the source of solvated electrons, x is the distance from the electrode, k is the rate constant of the reaction between the solvated electron and an acceptor molecule, c is the acceptor concentration, and D_S is the diffusion coefficient of the solvated electron.

In real systems, the emission current usually includes a component from the electrode reactions of the electron–acceptor complexes, and also of the products of their transformations in solution. These effects can distort the $I(\varphi)$ current–voltage characteristic, since the rate constant of the electrode reaction is (in general) a function of φ. However, if the electrode reactions of the products do not depend on φ in the region of interest, the current–voltage characteristic $I(\varphi)$ will be determined by $I_0(\varphi)$ and by the potential dependence of the source of solvated electrons.

This situation occurs for the acceptors N_2O and H_3O^+ (and for protons at $\varphi < -0.6$ V†), when the transfer of the second electron at the electrode–electrolyte interface involves the reduction of a hydroxyl radical or atomic hydrogen, and the emission current is simply doubled:

$$\begin{cases} N_2O + e_s^- \rightarrow N_2O^- \\ N_2O^- + H_2O \rightarrow N_2 + OH^{\cdot} + OH^- \end{cases}$$

$$\begin{cases} H_3O^+ + \bar{e}_s \rightarrow H + H_2O \\ H_{ad} + H_2O + e \rightarrow H_2 + OH^-, \end{cases}$$

where e_S is a solvated electron. N_2O and H_3O^+ have been used to investigate the detailed aspects of photoemission in solutions of electrolytes.

Some of the early workers[40,41], and also Heyrovsky[27], plotted their current–voltage and spectral measurements of the electrode photoeffect using ($\lg Q$, φ) and ($\lg Q$, $\hbar\omega$) co-ordinates, but Barker[3] and Delahay[17], who did not distinguish between photoemission into a vacuum and into a solution of electrolyte, used ($Q^{1/2}$, φ) and ($Q^{1/2}$, $\hbar\omega$) co-ordinates. (Here Q is the emitted charge). In both cases, the experimental results lay on a straight line over a limited region of potential. A more general law—the "five-over-two" law was first proposed[8,20] for the photoemission from mercury in the wave-length region 250–450 nm at potentials up to −0.7 V (relative to the point of zero charge) in acid solutions and up to −1.5 V (z.c.) in neutral or alkaline solutions containing nitrous oxide as an acceptor. It was shown that the current–voltage characteristics of the photoeffect "straighten out" when plotted in ($Q^{0.4}$, φ) co-ordinates‡ (Fig. 6). For solutions with different acceptor concentrations but constant ionic strength the straight lines intersect at one point on the potential axis.

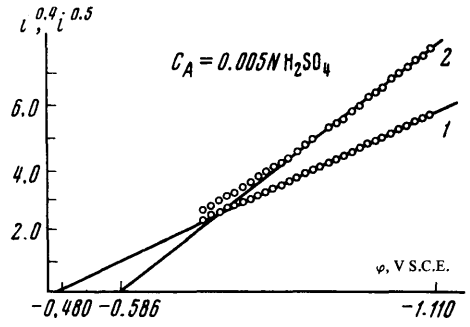


Figure 6. Current–voltage characteristic of the photoeffect in 0.005 N H_2SO_4 + 0.495 N K_2SO_4; λ = 405 nm: *1*) $i^{0.4}$ against φ; *2*) $i^{0.5}$ against φ.

Other workers[11,42] have also reported "linearisation" of the voltage–current characteristics for the photoemission effect on ($I^{0.4}$, φ) or ($Q^{0.4}$, φ) co-ordinates. The spectral dependence of the photoeffect gives a reasonably good straight line when plotted as $Q^{0.4}$ against $\hbar\omega$ (Fig. 7). The current–voltage curves for different $\hbar\omega$ values intersect the potential axis to give increments ($\Delta e\varphi$) proportional to the change in the energy of the light quantum ($\Delta\hbar\omega$), the proportionality coefficient being unity. Barker[3] finds the same value for the ratio $\Delta\hbar\omega/\Delta e\varphi$: the values between 2 and 3 reported by Heyrovsky[27] are probably due to secondary reactions which were ignored.

† Throughout this review, potentials are quoted relative to the saturated calomel electrode unless accompanied by a statement to the contrary.

‡ Reported deviations[22] from Eqn. (2) in the threshold region (at 436–579 nm) are probably due to thermal excitation processes in the metal, producing a photocurrent larger than required by Eqn. (2). The form of the threshold factor for $\frac{\hbar\omega - \hbar\omega_0 - e\varphi}{kT} \simeq 1$ is given in Ref. 6.

This means that the transmission coefficient of the barrier is sensibly constant within the dense part of the electrical double layer, which confirms the initial assumption of the Brodskii–Gurevich theory that the red photoemission threshold is linearly related to the electrode potential. Experiments on the frequency dependence of the photoemission by varying $e\varphi$ and $\hbar\omega$ together in such a way that the energy of the emitted electrons ($\hbar\omega - \hbar\omega_0 - e\varphi$) remains constant have shown that the function $\chi(\omega)$ in Eqn. (2) is independent of the medium into which photoemission occurs and is determined by the light absorption law in the metal. This experiment is not applicable to photoemission into a vacuum because of the frequency dependence of the threshold factor. The function $\chi(\omega)$ is found[22] to be a cubic hyperbola (Fig. 8): $\chi \sim \frac{1}{\omega^3}$. This result is consistent with the theory of photoemission assuming that the amplitude E of the light wave vector does not exhibit a singularity at the metal surface.

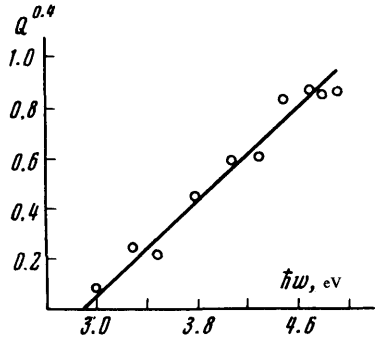


Figure 7. Spectral characteristic of the photoeffect in 0.1 N H_2SO_4; $\varphi = -0.8$ V.

When the energy of the emitted electrons is 1 eV and the energy of the absorbed photons is 3.52 eV, the quantum yield of the photoemission process is $(1.2 \pm 0.3) \times 10^{-4}$. This value agrees with the quantum yield of the photoemission into a vacuum[43] of electrons of 1 eV energy from a metal with a work function of 3.2–3.4 eV.

The work function from mercury into water W_0, calculated from spectral and current–voltage experiments by means of Eqn. (3), is 3.2 ± 0.05 eV (with H_3O^+ as the acceptor) or 3.13 ± 0.05 eV (with N_2O as the acceptor). This is close to the value of W_0 proposed by Frumkin from thermodynamic data[44] and to the "light quantum able to induce photocurrent at the point of zero charge" observed by Heyrovsky[27] with N_2O and H_3O^+ acceptors.

Many acceptors give current–voltage characteristics different from those described above for N_2O and H_3O^+ acceptors. The difference arises because the rate of the electrode reactions involving the products of electron capture by those acceptors varies with the potential[3,45].

We have shown[45] that in the presence of anionic acceptors both the current–voltage curve and the oscillographic $V(t)$ display of the photopotential depend on the Ψ' potential, on the acceptor concentration, and also on the ionic strength and on the pH of the solution. If the chemical reactions of the acceptors containing a captured electron are slow in comparison with the time of illumination, the trace of $V(t)$ does not follow the integral of the flash.

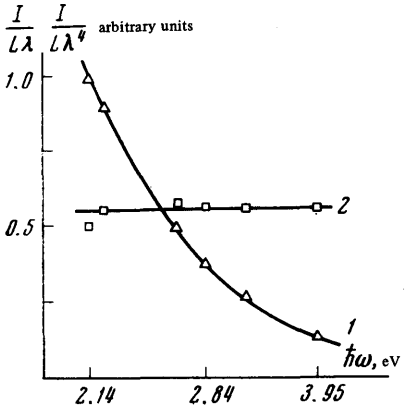


Figure 8. Frequency dependence of the photoemission current from mercury into 0.1 N KCl (acceptor N_2O); *1*) $I/L\lambda$; *2*) $I/L\lambda^4$; λ is the wave-length of the exciting light. Measured at constant $\hbar\omega - \hbar\omega_0 - e\varphi = 0.5$ eV.

Thus, in 1 M solutions of $NaNO_3$, KIO_3, and $K_2C_2O_4$ the current–voltage curves are S-shaped: at the more negative potentials the experimental points lie on straight lines in $Q^{0.4}(\varphi)$ plots, which can be extrapolated to give the shift from 3.2 eV of the threshold potential ($\Delta\varphi_b$).

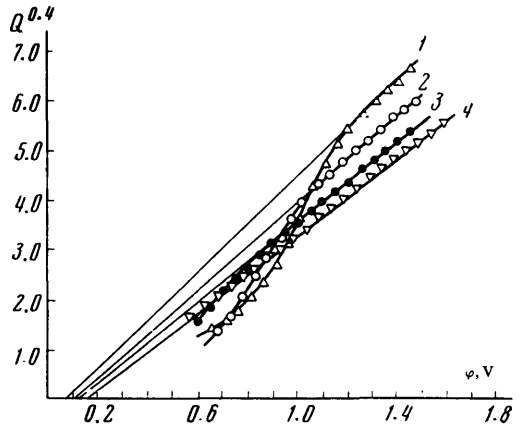


Figure 9. Emitted charge as a function of electrode potential in $NaNO_3$ solutions: *1*) M; *2*) 10^{-1} M; *3*) 10^{-2} M; *4*) 10^{-3} M (λ = 355 nm).

This can be negative ($\Delta\varphi_b = -0.4$ V for $NaNO_3$ and –1.1 V for $K_2C_2O_4$) or positive ($\Delta\varphi_b = 0.5$ V for KIO_3): see Figs. 9, 10, 11. However, when the contribution to the

photocurrent from secondary reactions can be ignored (acceptor concentration $10^{-3}-10^{-4}$ M, or alkaline medium) the function $Q^{0.4}(\varphi)$ becomes linear, and the work function approaches the value 3.2 V. In $K_2C_2O_4$ solutions we find, in addition to a cathodic photocurrent at negative potentials, an anodic photocurrent at $\varphi > \varphi_{z.c.}$, with a vanishingly small photoeffect in the intermediate potential region. KIO_3 solutions are distinguished by the presence of cathodic photocurrent at potentials more positive than the photoemission threshold.

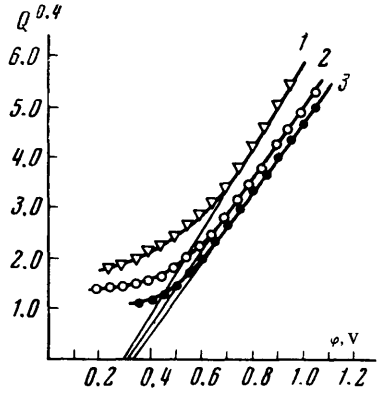


Figure 10. Emitted charge as a function of electrode potential in KIO_3 solutions: *1*) 10^{-1} M; *2*) 10^{-2} M; *3*) 10^{-3} M (λ = 355 nm).

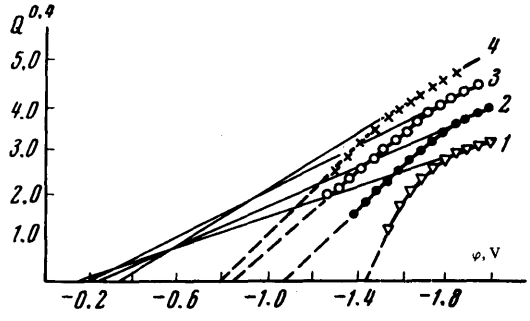


Figure 11. Emitted charge as a function of electrode potential in $K_2C_2O_4$ solutions: *1*) M; *2*) 10^{-1} M; *3*) 10^{-2} M; *4*) 10^{-3} M (λ = 355 nm).

The anodic photocurrent in oxalate solutions, and the cathodic photocurrent in iodate solutions at potentials more positive than the threshold potential, stem from the formation of a surface donor–acceptor complex. This can happen when $\varphi > \varphi_{z.c.}$, when the concentration of IO_3^- and $C_2O_4^{2-}$ in the electrical double layer suddenly increases. The anodic photocurrent is due to light-induced charge transfer to the electrode from the oxalate anion, which has a low ionisation potential, and the cathodic photocurrent to charge transfer (induced by light) from the metal to the iodate anion, which has a high electron affinity.

This conclusion was reached from a study of polarisation selectivity, an important feature of the surface photoeffect. This effect, associated with the polarisation of light absorption in metals, follows from the condition of conservation of momentum, which can be satisfied in the surface photoeffect only in a direction perpendicular to the surface[46]. Conversely, in the photocurrent model involving ionisation of surface complexes, polarisation selectivity seems improbable, since the binding energy of the complex is comparable to the molecular vibration energy, and complex formation leads to the interaction of vibrational states of different symmetry[47].

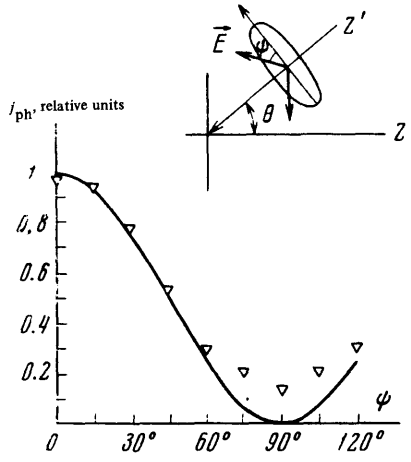


Figure 12. Polarisation dependence of the photoeffect in 0.1 N K_2SO_4 (φ = −1.4 V); z is the direction normal to the electrode surface, θ is the angle of incidence of the light, E is the vector of the electric component of the electromagnetic wave, ψ is the polarisation angle in the incidence plane (z,z'), j_{pH} is the measured photocurrent, the symbol ▽ denotes experimental points, the full line is a plot of $\cos^2\psi$.

Polarisation selectivity of the electrode photoeffect was predicted by Brodskii and Gurevich[6] and experimentally demonstrated by Korshunov and coworkers[10]. A decrease in photocurrent with a decrease in the normal component of the electric vector was observed at negative potentials in all the solutions examined (H_3O^+, N_2O, and anion acceptors). The polarisation ratio varied between 2.5 and 7, depending on the angle of incidence of the light on the photocathode (Fig. 12).

Since for the linear photoeffect $j \sim E_{\parallel}^2 = E_0^2 \sin^2\theta \cos^2\Psi$ (where θ is the angle of incidence, Ψ is the polarisation angle of the electric vector E of the electromagnetic wave in the incidence plane, j is the photocurrent), the angular dependence of the photocurrent is given by

$$j = j_0 \sin^2\theta \cos^2\psi, \qquad (4)$$

which satisfactorily describes the observed polarisation behaviour.

Polarisation of the cathodic photocurrents has been observed also in $H_2C_2O_4$ and $K_2C_2O_4$ solutions, but the

anodic photocurrents in these solutions show practically no polarisation selectivity.

The polarisation selectivity of the cathodic photocurrent is proof that the photoeffect is the result of photoemission of electrons from the metal into the solution. Conversely, the lack of selectivity of the anodic photocurrent can be taken as evidence that the photoeffect at $\varphi > \varphi_{z.c.}$ arises from light-induced electron transfer in the surface complex from the oxalate anion (which has a low ionisation potential) to the metal.

IV. STATUS OF THE "FIVE-OVER-TWO" LAW AND OF THE DISTRIBUTION FUNCTION OF SOLVATED ELECTRONS

The good qualitative and quantitative agreement between the spectral and current–voltage characteristics of the electrode photoeffect and Brodskii and Gurevich's photoemission theory[6] is evidence that we are dealing with an emission phenomenon, but it does not prove that the "five-over-two" law is in any way a fundamental one.

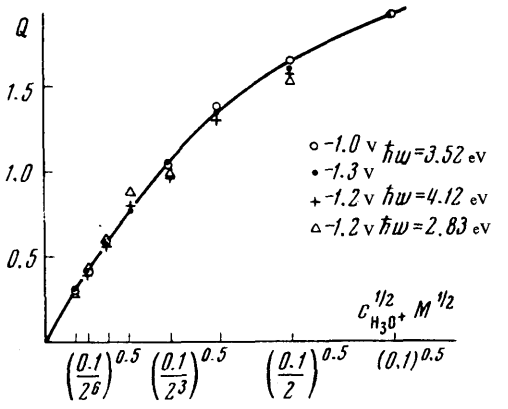


Figure 13. Emitted charge as a function of H_3O^+ acceptor concentration for different φ and $\bar{n}\omega$. The scale of Q is chosen so as to bring into coincidence the points for the maximum acceptor concentration ($c_{H_3O^+} = 0.1\ N$, far right of the curve).

Thus, as already stated, the experimental $I(\varphi)$ and $I(\bar{n}\omega)$ plots are determined not only by the characteristics of the emission current, but also by the dependence upon the energy of the emitted electrons of the distribution function describing the source of solvated electrons. Since the residence time of a solvated electron is much greater than its formation time, the trapping process may be described in terms of an initial distribution of solvated electrons, produced by the photoemission. With this assumption, the variation of the photocurrent (or emitted charge) with acceptor concentration at different photon energies and electrode potentials can be used to arrive at the form of the distribution for different initial electron energies. The charge emitted from mercury into an electrolyte solution under pulse illumination has been studied[48] over a range of concentrations of the electron acceptors H_3O^+, N_2O, and NO_3^-. In the absence of secondary reactions by the electron-filled acceptors, the experimental $Q(c)$ curve is related to the function of the source of solvated electrons $f(x)$ by Eqn. (3).

Fig. 13 shows a plot of $Q(c)$ for H_3O^+ at different values of φ and $\bar{n}\omega$. The arbitrary scale of Q is normalised so as to make the experimental Q values at the maximum acceptor concentration (0.1 M) coincide.

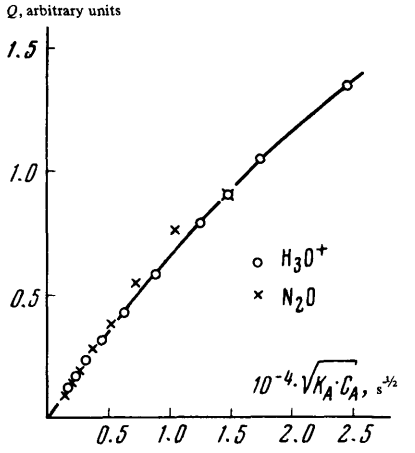


Figure 14. Emitted charge as a function of the parameter $\sqrt{kc}$.

Within experimental error (±5%), the measurements are described by a single curve, i.e. the source function is independent of the emitted electron energy over the range 0.5–1.6 eV. Measurements of Q as a function of the capture efficiency $(\kappa c)^{1/2}$ for different acceptors shows that the source function is also independent of the nature of the acceptor (Fig. 14). From these results we may conclude that the source function is finite at $x = 0$ and can be expressed by the summation

$$f(x) = \sum_i \left(\frac{kc}{D_s}\right)^{1/2} e^{-x/x_{0i}} \qquad (5)$$

Because the experimentally accessible range of $(\frac{kc}{D_s})^{1/2}$ measurements is limited, only the characteristic length x_0 of the distribution can be determined. If the source function is exponential,

$$\frac{Q(c)}{\sqrt{c}} + Q(c)\sqrt{\frac{k}{D_s}}x_0 = Q_0\sqrt{\frac{k}{D_s}}x_0\ , \qquad (6)$$

and a linear relation between $\frac{Q}{\sqrt{c}}$ and Q should be observed.

Eqn. (6) is satisfied at high values of Q, i.e. at high acceptor concentrations. For $D_S = 5\times10^{-5}$ cm^2 s^{-1} [3] and $k = 8.7\times10^{10}$, the results for H_3O^+ give $x_0 = 16$ Å (Fig. 15).

However, at lower values of Q we observe deviations from linearity: at $c \leqslant 5\times10^{-4}$ M for H_3O^+ and at $c < 10^{-3}$ M for NO_3^-. With N_2O ($c_{max} = 2.5\times10^{-2}$ M), $Q/\sqrt{c}$ is practically independent of Q. The deviation from linearity of the function $\frac{Q}{\sqrt{c}}(Q)$ may result from a decrease

in the rate constant of the reaction between the solvated electron and the acceptor, as indicated by radiation-chemical data[49,50], or alternatively it may be due to the failure of Eqn. (6) to provide a satisfactory approximation at small values of x. At low acceptor concentrations, when the major contribution to Q comes from the tail of the source distribution function, the observed non-linearity suggests that $f(x)$ falls off more sharply at large values of x than given by Eqn. (6) with $x_0 = 16$ Å.

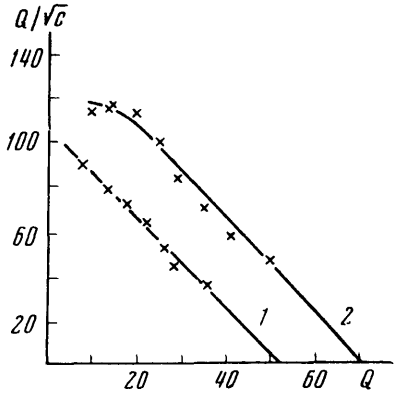


Figure 15. Plots of $Q/\sqrt{c}$ against Q for H_3O^+. Ionic strength held constant (1 N) by adding Na_2SO_4; $\lambda = 300$ nm: *1*) $\varphi = -1.0$ V; *2*) $\varphi = -1.2$ V.

The independence of the source function upon the energy of the emitted electrons in the range $0.5 \leq E \leq 1.5$ eV is also confirmed by the good fit to the "five-over-two" power law of the current–voltage curves at different acceptor concentrations. The results justify the conclusion that the experimentally observed "five-over-two" law has a fundamental significance, i.e. that the Brodskii–Gurevich model[6] of photoemission into a solution is essentially correct. This conclusion is also relevant to the MDM structure (metal–dielectric–metal), for which the photoemission model is similar to the model of photoemission into electrolyte solutions[7], with similar deviations form Fowler's law[51–56].

The escape distance of the electron from the electrode (16 Å for water) is consistent with the mean free path of the secondary electrons produced in the radiolysis of aqueous solutions, for which the values 16 Å and 30 Å have been obtained[57,58] by an analysis of the diffusion kinetics of the radiolysis process.

The value $x_0 = 16$ Å suggests that the main scattering mechanism for low-energy electrons is inelastic interaction. It may be assumed that the energy scattering process involves vibrational relaxation (for water, the relevant vibrational levels are 0.198, 0.474, and 0.488 eV)[59].

As already stated, x_0 has been evaluated on the assumption that the electron becomes solvated before being captured by an acceptor, but the value of x_0 is too small to exclude the possibility of direct capture of unsolvated ("dry") electrons. The diffusion equation holds true if the mean free path, determined by scattering processes (e.g. as a result of vibrations), under equilibrium conditions is larger than the wave packet[60]

$$\lambda = \frac{h}{(3m_0kT)^{1/2}} = 10\ \text{Å} \qquad (7)$$

so that the capture of "dry" electrons by acceptors, followed by release of the electrons to the electrode, can be treated as a diffusion process only at distances greater than λ, whereas x_0 is comparable to λ in magnitude. The relative contribution of solvated and "dry" electron interactions with the acceptor can be evaluated from the kinetics of electron release for irradiation times of the order of the diffusion time of solvated electrons to the electrode (10^{-8}–10^{-9} s).

The kinetics of the photocurrent integral have been studied with a nitrogen laser: in a 1 N H_2SO_4 solution the photocurrent integral is ($\Delta t = 10^{-8}$ s) within experimental error identical with the integral of the light pulse, recorded with a fast photomultiplier. The upper limit of the characteristic length x_0 follows directly from this result: for $\Delta t = 10^{-8}$ s, $x_0 < 70$ Å.

According to Wolf and coworkers[61], protons do not interact with "dry" electrons. It appears[61] that the observed value of x_0 relates to solvated electrons. At proton concentrations below 10^{-2} M (in a 1 N solution) the $V(t)$ curve includes a slowly rising portion of 100–150 ns duration which accounts for ~ 20% of the maximum signal amplitude. In N_2O solutions ($C_a \leq 2 \times 10^{-2}$ M) a signal of this form is observed at all acceptor concentrations. This slow increase needs to be investigated further in order to establish whether it is the results of electrode or of bulk reactions of the filled acceptors, or whether it is due to the variation of x_0 with acceptor concentration.

V. TUNNELLING OF EMITTED ELECTRONS THROUGH THE POTENTIAL BARRIER AT THE INTERFACE

One of the most significant differences between photoemission into electrolyte solutions and photoemission into a vacuum is the linear dependence of the long-wave limit of the photoeffect on the electrode potential, due to the fall in potential over distances of atomic dimensions from the metal surface. It follows that tunnelling penetration of the barrier by electrons having an energy lower than the work function by an amount $e\varphi$ becomes possible.

The tunnelling model satisfactorily describes photoemission into dilute solutions and solutions containing surface-active compounds. In the former case, in addition to the potential drop across the dense part of the double layer, we have to consider the Ψ' potential, acting over distances of tens or hundreds of Ångstroms and therefore unlikely to permit tunnelling. Thus, for the case of photoemission into dilute solutions the full potential drop in Eqn. (2) should be replaced by the potential drop across the dense part of the double layer, through which the emitted electrons are able to tunnel:

$$I_0 = L(t)\chi(h\omega - h\omega_0 - e\varphi + e\psi')^{1/2}, \qquad (8)$$

and dilute solutions should show deviations from linearity in the $Q^{0.4}$ versus φ plots, due to the $\Psi'(\varphi)$ variation.

Eqn. (8) has been tested[18] in potassium sulphate solutions of concentration between 10^{-1} and 10^{-5} N.

In Fig. 16 the Ψ' potentials given by Eqn. (8), corresponding to the horizontal shift of the $Q^{0.4}(\varphi)$ curves in K_2SO_4 solutions with increasing dilution (with respect to the straight line for the concentrated solutions drawn so as to intersect the dilute solution curve at the point of zero

intersect the dilute solution curve at the point of zero charge), are compared with the Ψ' potentials given by the Gouy–Chapman theory for electrolyte solutions without specific adsorption. Similar results have been obtained in acid solutions[18]. Other workers[11,42] also conclude that a correction for the Ψ' potential must be applied to the photocurrent equation, but in their view the correction should be smaller than Ψ'.

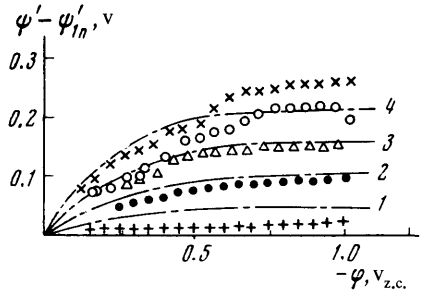


Figure 16. Shift of current–voltage curves in dilute solutions, relative to 1 N K_2SO_4 (N_2O acceptor). The broken curves correspond to the theoretical ψ' potential: *1*) 0.1 N; *2*) 0.01 N; *3*) 0.001 N; *4*) 0.0001 N.

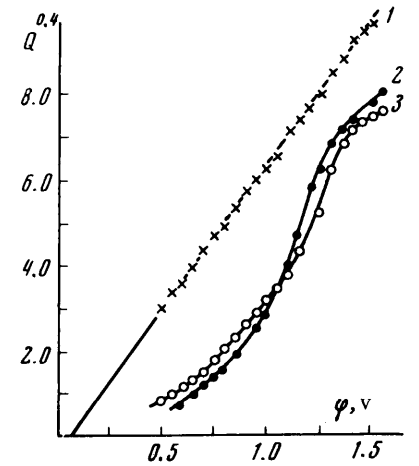


Figure 17. Current–voltage curves in solutions of caprylic and enantic acids: *1*) base solution 0.1 N KF; *2*) 0.1 N KF + 0.01 M $C_9H_{17}COOH$; *3*) 0.1 N KF + 0.01 M $C_6H_{11}COOH$.

In dilute solutions containing an acceptor, as well as in concentrated solutions, the rise time of the photopotential is the same as the duration of the light pulse, and the reverse diffusion current of solvated electrons follows any change in light intensity. In the absence of acceptors, however, the shape of the pulse changes: the initial rise is followed by a 30% fall of photopotential after approximately 5×10^{-4} s, and a more gradual decay with a time constant $RC = 0.1$ s. A signal of this form is consistent with hindered reverse flow of the solvated electrons to the electrode: a rate constant for the interaction between e_S and a water molecule agreeing with the published value[62] (2×10^3 s^{-1}) has been deduced from these data. The slope of the linear portion of the $Q^{0.4}(\varphi)$ plot increases with decreasing ionic strength of the solution, irrespective of the presence or absence of acceptors and of the kind of acceptor present, in contrast to the predictions of the theory of ionic reactions in solution[63]. This result evidently follows from the decrease in the number of electrons returning to the electrode in dilute solutions, caused by the effect of the Ψ' potential on the source function.

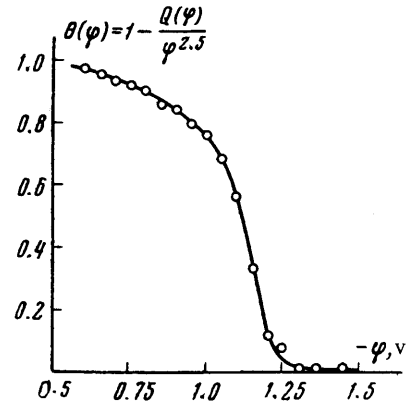


Figure 18. Coefficient $K = 1 - Q/\Delta\varphi^{5/2}$ against electrode potential in a solution of enantic acid.

The results for solutions of specifically adsorbed anions (Cl^-, Br^-, I^-) containing propanol and butanol[64,65] are in keeping with the dilution experiments. The photoemission current–voltage curve is linear when plotted as $Q^{0.4}(\varphi)$, and the work function is the same as in the solution without adsorbable ions. The tunnelling distance of the electrons is greater than the thickness of the dense part of the double layer (in NaF solution), but it is not more than 10 Å. In solutions containing surface-active compounds (s.a.c.) with molecules larger than 10 Å the $Q^{0.4}(\varphi)$ plots are S-shaped (see Fig.17)[65]. The function $\theta(\varphi) = 1 - \dfrac{Q}{(\hbar\omega - \hbar\omega_0 - e\varphi)2.5}$, which describes the deviation of the current–voltage curve from the "five-over-two" law, can be correlated with the coverage of the electrode surface by s.a.c. (Fig. 18), which suggests tunnelling of the electrons through surface sites not covered with adsorbed molecules. When s.a.c. are introduced into electrolyte solutions, it is necessary to allow for the effect of the adsorption Ψ' potential on the kinetics of the electrode reactions involving the species produced by the reaction between solvated electrons and acceptors (e.g. H_3O^+).[65]

VI. PHOTOEMISSION FROM METALS INTO ELECTROLYTE SOLUTIONS AS A METHOD OF STUDYING FAST REACTIONS

Photoemission from a metal into a solution has been used successfully to determine the rates of fast chemical reactions. This application of the photoemission method

is based on the separation (in time, or in terms of dependence on the electrode potential) of the primary photoemission current I_0 from the secondary currents resulting from electrode reactions of the dissolved species containing a captured emitted electron. Since photoemission itself is practically instantaneous ($\tau < 10^{-11}$ s), and the characteristic thermalisation time is even smaller, the time during which primary current flows is exactly the same as the time of illumination. The time associated with the reverse flow of solvated electrons to the electrode is of the order of $x_0^2/D_S \simeq 10^{-10}$ s, so that for illumination times $t \gg x_0^2/D_S$ the charge added to the solution by the photoemission current is

$$Q = Q_0 \frac{\left(\frac{kc}{D_s}\right)^{1/2} x_0}{1+\left(\frac{kc}{D_s}\right)^{1/2} x_0} \qquad (9)$$

It follows from Eqn. (9) that the electron-capture reaction can be investigated by measuring the function $Q(c)$. The upper limit of the illumination time ($T = 10^{-8}$ s) is set by the need to avoid complications from the relatively slow subsequent transformations of the acceptor. These slower reactions can be studied by using longer exposure times. Studies of reactions of this type, with nitrate or oxalate ions as the acceptors, have been reported[66,67].

The irreversible reactions of these acceptors involve the following scheme:

$$e_s^- + A \xrightarrow{k} A_s^-$$
$$\text{(a)}\ A_s^- \xrightarrow{\kappa_1(\varphi)} A + e_M^-$$
$$\text{(b)}\ A_s^- \xrightarrow{k_2} A_1^{\cdot} + A_2$$
$$A_2 + e_M^- \xrightarrow{\kappa_2} A_2^-$$

where A is the acceptor molecule, e_S^- is the hydrated electron, A_S^- is an acceptor molecule containing a trapped electron, A_1 and A_2 are products derived from an acceptor molecule with a trapped electron, k is the rate constant of the reaction between a solvated electron and an acceptor molecule, κ_1 and κ_2 are the rate constants of the electrode reactions of A_S^- and A_2, k_2 is the rate constant for the decomposition of A_S^-. (In the range of potentials relevant to this work, κ_2 is usually large and independent of φ.)

The processes which consume A_S^- (decomposition in solution and oxidation at the electrode) are competing reactions, and can be separated by varying the electrode potential. In the potential region where κ_1 is small the electrode current is given by

$$I = I_0 - I_1 + I_{A_2}$$

When $k_2^{-1} \gg x_0^2/D$, the charge collected by the electrode due to the electrode reaction of A_2 particles is given by

$$Q_{A_2}(t) = \frac{D_{A_2} \cdot k_2}{2} \int_0^t \exp\left(-\frac{k_2 t'}{2}\right) \left\{I_0\left(\frac{k_2 t'}{2}\right) - I_1\left(\frac{k_2 t'}{2}\right)\right\} dt' \qquad (10)$$

where I_0 and I_1 are Bessel functions.

It is evident from Eqn. (10) that Q_{A_2} increases initially but tends to a constant value with a time-constant k_2. Part of the observed photocurrent ($I_0 - I_1$) follows instantaneously the intensity of the exciting light. Hence, we can distinguish the signal due to the electrode reaction of the A_2 particles from the background of the observed photocurrent, and we can evaluate k_2 (Fig. 19*a*). Thus, the lifetime of the hydrated NO_3^{2-} anion is $\tau = k_2^{-1} = 10^{-4}$ s, in good agreement with the value determined by pulse radiolysis[50].

When reactions (a) and (b) are both significant, the current–voltage characteristic of the observed photocurrent ($I = I_0 - I_1 - I_{A^-} + I_{A_2}$) is determined by the current–voltage characteristics of the individual components. For an exponential source function $f(x) = \frac{I_0}{x_0} \exp(-x/x_0)$ in the steady state,

$$I = \frac{I_0}{x_0}\left\{\frac{\lambda_1}{(\lambda_0+\lambda_1)\lambda_0} - \frac{\lambda_1^2 \varkappa_1}{[\varkappa_1 + (k_2 D_{A_2})^{1/2}](\lambda_0+\lambda_1)(\lambda_1+\lambda_2)(\lambda_0+\lambda_2)} + \right.$$
$$+ \frac{\lambda_1^2 \lambda_2}{2(\lambda_0^2-\lambda_1)^2}\left[\frac{(k_2 D_{A_2})^{1/2} - \varkappa_1}{(k_2 D_{A_2})^{1/2} + \varkappa_1} \cdot \frac{\lambda_0 - \lambda_1}{(\lambda_1+\lambda_2)(\lambda_0+\lambda_2)\lambda_2} + \right.$$
$$\left.\left. + \frac{1}{\lambda_1(\lambda_1+\lambda_2)} - \frac{1}{\lambda_0(\lambda_0+\lambda_1)} - \frac{1}{\lambda_1\lambda_2} - \frac{1}{\lambda_0\lambda_2}\right]\right\} = I_0 f(\lambda_0, \lambda_1, \lambda_2, \varkappa_1) \quad , \qquad (11)$$

where

$$\lambda_1 = \left(\frac{kc}{D_s}\right)^{1/2}; \quad \lambda_2 = \left(\frac{k_2}{D_{A_2}}\right)^{1/2}; \quad \lambda_0 = x_0^{-1} \quad .$$

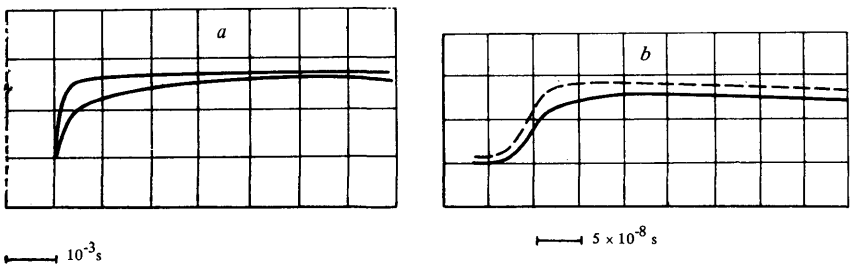


Figure 19. Photopotential in the presence of reactions in solution induced by the emitted electrons: (*a*) 1 *N* $NaNO_3$, upper and lower trace for $\varphi = -1.0$ and -1.4 V respectively; (*b*) 1 *N* $Na_2C_2O_4$, broken line is the integral of the light pulse.

Since λ_0 and λ_2 can be determined from Eqns. (9) and (10), we can evaluate the parameters of the electrode reaction of A^- by comparing the experimental function $\theta(\varphi) = Q(\varphi)(\Delta\varphi)^{-5/2}$, which gives the deviation from the "five-over-two" law, with the theoretical function $f(\lambda_0, \ldots \kappa_1)$. The function $f(\lambda_0, \lambda_1, \lambda_2, \kappa)$ is plotted against the parameter κ in Fig. 20 for $\lambda_0 = 10^6$ cm^{-1}, $\lambda_1 = 1.7 \times 10^7$ cm^{-1}, $\lambda_2 = 1.7 \times 10^4$ cm^{-1}, together with the experimental function $\theta(\varphi) = Q(\varphi)(\Delta\varphi)^{-5/2}$. The transfer coefficient $\alpha = 0.2$ and the constant

$$A = \ln k_s + \frac{\alpha e}{kT}\varphi_p = -7.6$$

can be determined by comparing the theoretical and the experimental curve.

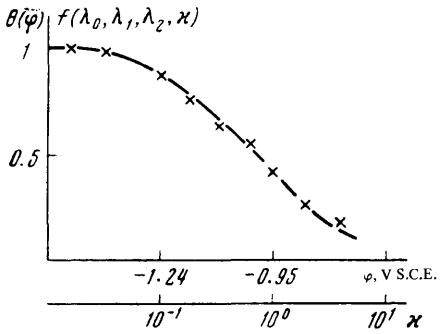


Figure 20. Comparison of the theoretical $f(\lambda_0, \lambda_1, \lambda_2, \kappa)$ (full line) and of the experimental $\theta(\varphi)$ functions.

The function $\theta(\varphi)$ in oxalate solutions is also S-shaped, with an inflection point around -1.65 V in 1 N solutions. As in the case of NO_3^- solutions, the shape of the function can be attributed to oxidation (at the electrode) of the CO_2^- ion produced from the capture of an emitted electron by an oxalate anion[27]. The resulting CO_2^- ion is oxidised at the electrode, or alternatively it can undergo chemical changes in solution when $\varphi < -1.7$ V and the rate constant of the electrode reaction is small. Since no changes in the oscillogram were noted in this region of potential, only the upper limit of the lifetime of the hydrated $C_2O_4^{3-}$ anion could be estimated ($\tau < 2 \times 10^{-6}$ s, see Fig. 19*b*).

VII. WORK FUNCTION OF ELECTRONS FROM METALS INTO POLAR SOLVENTS

The work function for the emission of electrons into water has been measured[68,69] for the following metals: Hg, Zn, Cd, Pb, Tl, Ga, Sn, Bi, Al, In, Sb, Pt, Ni, Fe, Cu, Ag, Au. With the metals whose polarisability is ideal over a sufficiently wide range, i.e. Bi, Ag, Pb, Zn, Sn, Sb, Hg, the relationship $Q^{0.4}(\varphi)$ is linear over the whole of the working range of potential, as shown in Fig. 21. The other metals have a narrower linearity region. The potential, extrapolated with respect to the reference electrode, is the same for all the metals: 0.15 ± 0.1 V S. C. E. The same conclusion was reached independently[11] for In and Tl amalgams.

The work functions of the metals, referred to published values[70] of the point of zero charge, are listed in Table 1. In most cases the difference between the water and the vacuum work function lies in the range 1.35 ± 0.15 eV.

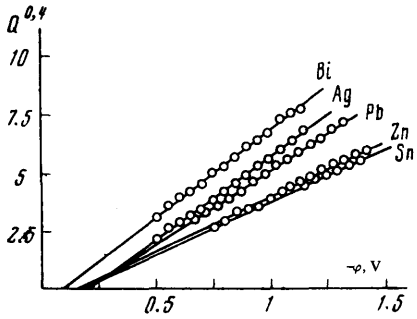


Figure 21. Emitted charge against electrode potential for various metals (0.1 N NaF + N_2O, λ = 355 nm).

The variation of the work function in water with zero-charge potential (relative to the normal hydrogen electrode) is shown in Fig. 22 for a number of metals. (The zero-charge potentials φ_0 are known with adequate precision for these metals.) The experimental dependence is described by the equation

$$\varphi_0 = h\omega_0 - 3.44 \qquad (12)$$

Table 1.

Metal	Work function	Metal	Work function
Cd	2.70	Tl	2.87
Zn	2.77	In	2.90
Ag	2.77	Ga	2.90
Pb	2.91	Al	3.00
Sn	2.94	Ni	3.25
Bi	2.97	Fe	3.02
Hg	3.15	Sb	2.82
Cu	3.46	Pt	3.50
Au	3.72		

This equation allows us to convert the conventional potentials relative to the normal hydrogen electrode into the energy (relative to the free electron in a vacuum) needed to remove an electron from the metal. The constant, equal to the work function at zero hydrogen potential, can be equated to the standard hydrogen potential in electron-volts.

It should be noted that it is much simpler in practice to determine the work function from a metal into an electrolyte solution than into a vacuum, since surface states (which are known to affect the work function in vacuo) have no effect on the photoemission threshold in electrolyte solutions (see previous Section). Hence, $\hbar\omega_0$ values can be measured without special surface treatment provided that the light absorption and the electron emission take place in the metal itself.

Photoemission has been studied in polar solvents other than water in order to increase our understanding of the energetics of the process. The solvents examined include alcohols and dimethylformamide (DMF): their molecules have a capture efficiency for emitted electrons and for the products of their interaction with acceptors (H or OH') higher than the capture efficiency of water, a feature which complicates the measurement of work function.

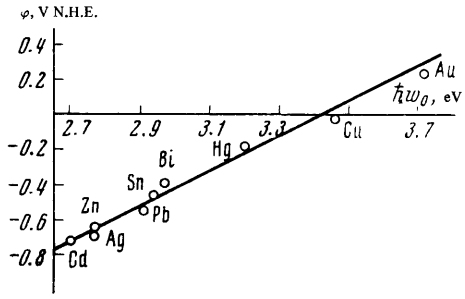


Figure 22. Work function of metals in water against potential at the point of zero charge.

Photopotential oscillograms of the normal form, and linearity of the $Q^{0.4}(\varphi)$ current–voltage characteristics, were taken as criteria for the correct choice of work function measurement conditions. With alcohols, these criteria were satisfied by using H^+ as the acceptor, and with DMF by using N_2O at sufficiently negative potentials ($\varphi < -1.1$ V S. C. E.).[69] The work functions from mercury into these solutions are given in Table 2.

Table 2. Work function of mercury in various solvents.

Solvent	$\hbar\omega_0$, eV	$W_0 - \hbar\omega_0$, eV
H_2O	3.15	1.35
CH_3OH	3.6	0.90
C_2H_5OH	3.75	0.75
DMF	3.95	0.55

The difference between the vacuum work function and the work function in the above solvents is much less than the intrinsic energy of a polaron in these media (over 3 eV). This suggests that only the electronic part of the polarisation is able to keep pace with the motion of the emitted electron at the moment when it enters the medium, and therefore $W_0 - \hbar\omega_0$ should correspond to the intrinsic energy of the electronic polaron in the medium. The slow part of the polarisation begins to relax only after the electron has been slowed down to thermal velocity ($\tau \geq 10^{-13}$ s). The calculated energies[72-74] of the electronic polaron ($E = e^2/d(1 - \varepsilon_\infty^{-1})$, where $d \simeq V_0^{1/3}$, V_0 is the volume occupied by one molecule, and ε_∞ is the optical dielectric permeability) correlate with the observed decrease of $W_0 - \hbar\omega_0$ in the sequence: water, alcohols, DMF.

Thus, the position of the conduction band in these solvents can be deduced from measurements of the work function $\hbar\omega_0$.

VIII. MULTI-PHOTON PHOTOEMISSION FROM MERCURY INTO ELECTROLYTE SOLUTIONS AND PULSE HEATING OF THE SOLUTION

When the wave-length of the exciting light is much longer than the threshold for one-electron photoemission two types of process are observed: 1) photocurrents arising from the pulse heating of the layer of solution in contact with the electrode[8] and 2) photoemission currents due to multi-photon absorption of light in the metal[9].

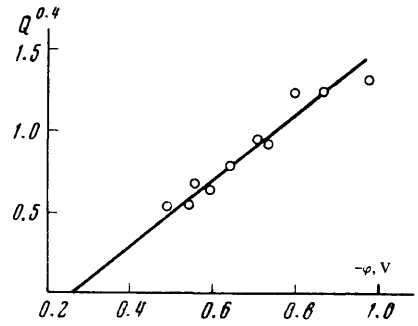


Figure 23. Emitted charge against electrode potential in 0.1 N $HClO_4$ illuminated with pulses from a ruby laser.

Table 3. Comparison of published[70] zero-charge potentials with the values obtained by the heating current method.

Metal	Potential of sign inversion	Assumed (Ref.70) values of φ_0, eV
Hg	−0.19	−0.19
Cd	−0.74	−0.72
Pb	−0.57	−0.56
Bi	−0.42	−0.40
Pt	0.10	0.11–0.19
Sn	−0.52	−0.46
Ag	−0.66	−0.70

The emission currents and the heating currents at a negatively charged mercury surface have different signs and are easily distinguished. With ruby laser light ($\hbar\omega = 1.785$ eV) the emitted charge is $Q \sim L^2$, where L is the light intensity. The current–voltage characteristic is linear in $Q^{0.4}(\varphi)$ coordinates (Fig. 23). The work function agrees with the single-photon value if the appropriate correction is made to Eqn. (2):

$$Q^{0.4} \sim 2h\omega - h\omega_0 - e\varphi. \qquad (13)$$

The characteristics observed indicate that in this case photoemission is caused by two-photon absorption in the metal. The magnitude of the emitted charge ($Q = 2.4 \times 10^{-7}$ C cm^{-2} at $\varphi = -0.5$ $V_{z.c.}$) is consistent with the theory of two-photon photoemission[75].

Upon illumination with neodymium laser light ($h\omega$ = 1.18 eV), $Q \sim L^3$, and the photoemission is associated with the absorption of three photons. The emitted charge is $Q = 8 \times 10^{-9}$ C cm^{-2} at $\varphi = -0.5$ $V_{z.c.}$.

The temperature gradient of the electrode potential on pulse heating ($10^{-3}-10^{-2}$ V deg^{-1}) is numerically equal to the temperature dependence of the double layer capacity ($\frac{1}{C}\frac{\partial Q}{\partial T} = 10^{-3}-10^{-2}$ V deg^{-1}).[76]

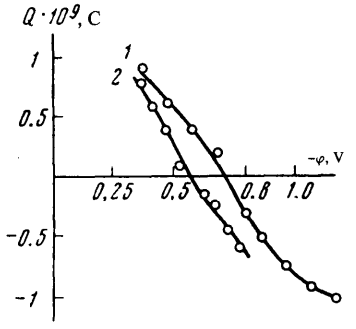


Figure 24. Integral of the heating photocurrent against electrode potential (0.1 *N* NaF): *1*) Cd; *2*) Pb.

The characteristics of the heating photocurrents due to the decrease in charge density of the double layer upon irradiation of the interface with pulses of long-wave light can be used to measure the point of zero charge for metals[8,77]. When $\varphi > \varphi_{z.c.}$ the heating photocurrents have a cathodic sign; on lowering the potential the photocurrent passes through zero and becomes anodic for $\varphi < \varphi_{z.c.}$ (see Fig. 24). The potentials for zero heating current, measured in this way, are consistent with the published points of zero charge for the metals[77] (Table 3).

The main advantages of this method are the ease of application to solid electrodes and the direct indication of the sign of the charge on the electrode surface.

IX. CHARGE TRANSFER THROUGH THE ELECTRODE–SOLUTION INTERFACE DURING PHOTOCHEMICAL REACTIONS IN SOLUTIONS

We have so far been concerned with the photocurrents produced by illumination of the metal–electrolyte interface. The solution was assumed to be unaffected by light, and the photocurrent was assumed to arise from emission of electrons from the metal or from ionisation of the surface donor–acceptor complexes involving the electrode as one of the components.

Photocurrents can also be produced by photochemical reactions in solution, or on the electrode surface, which are able to produce electrochemically active particles (electronically excited molecules, radicals, or stable molecules). The surface reaction is almost impossible to distinguish from ionisation of a surface complex. Photocurrents have been observed in aqueous and non-aqueous solutions of organic (aldehydes, ketones[78-80], quinones[81-83], dyes[84-86]) and inorganic compounds (metal ions of variable valency[87]). These photochemically and electrochemically active systems are highly relevant to the study of biologically important respiratory and photosynthetic processes[88,89], and also in the development of solar energy conversion devices[90,91]. Photoelectrochemistry was first widely used as a method of investigation by Berg[92], who used steady illumination in conjunction with polarography. The kinetics of formation and decay of photochemically-generated radicals were studied by solving the diffusion equation at a dropping electrode with allowance for photochemical reactions in solution and for the disappearance of radicals by various assumed mechanisms. Stable particles accumulate in the medium, and can be identified polarographically[92-95]. The mechanism of photo-reduction of quinoid compounds in aqueous solutions, and the nature of the photopotential, have been studied[92-95] by analysing the kinetic curves for the stable photolysis products constructed from polarographic data. The kinetic curve for the irreversibly formed photolysis products is S-shaped, showing that the formation reaction involves an intermediate step, and that the primary act consists in reversible photo-reduction (H_2O and OH^- being the electron donors). The photopotential varies linearly with the logarithm of the ratio of oxidised to reduced form of the compound, pointing to the reversible photolysis products[98] being the main potential-determining species in the system.

Berg[99] gave the first formulation of the problems concerning the study of excited states by electrochemical methods. The earlier workers[99-101] failed to detect photocurrents associated with electrode reactions of excited molecules because their experimental technique was inadequate: the excited states were formed too far from the electrode, and suffered deactivation before reaching the electrode by diffusion. However, Maricle and Maurer[102] were successful: they illuminated solutions of rubrene and zinc tetraphenylporphyrin in DMF through an optically transparent electrode (a film of SnO_2 deposited on glass).

For rubrene in the range of potential where the redox reaction does not give a dark current ($E_{1/2}^{Ox} = 0.95$ V, $E_{1/2}^{Red} = -1.34$ V S. C. E.), cathodic polarisation produced initially an anodic and then a cathodic photocurrent, the change of sign corresponding to a potential φ half-way between $E_{1/2}^{Ox}$ and $E_{1/2}^{Red}$. The observed photocurrent was assigned to the electrode oxidation or reduction of the rubrene singlet, whose energy is close to $E_{1/2}^{Ox} - E_{1/2}^{Red} = 2.29$ eV.[101] Illumination of zinc tetraphenylporphyrin revealed a triplet state ($E_T < E_{1/2}^{Ox} - E_{1/2}^{Red}$). Photocurrents due to the discharge of excited pyrene molecules at a semi-transparent gold electrode have also been observed[102].

Solutions of aromatic hydrocarbons in aprotic solvents are very interesting from the viewpoint of the electrochemistry of excited states, since they present the opposite problem: the electrochemical generation of excited states (electrochemiluminescence). The phenomenon has been observed during a.c. electrolysis (35–400 Hz) of rubrene, phenanthrene, pyrene, pyrylene, naphthacene, anthracene, 9,10-diphenylanthracene, 9,10-dimethylanthracene, and 3,4-benzpyrene in acetonitrile, benzonitrile, and DMF solutions with inert (usually platinum) electrodes and quaternary salts as supporting electrolytes[103-110]. Durst and Taylor[87] observed photocurrents due to excited ions at the reduction potentials of Ni^{2+} and Co^{2+}, but they did not allow for the photoemission current from the mercury electrode.

The most promising method of investigating metastable states is pulse illumination in conjunction with the relaxation methods of electrochemical kinetics[79,96]. The condition for observable photocurrent is that the lifetime of the metastable state (τ_0) should be comparable with the time of diffusion from the illuminated region to the electrode and with the time of the electrode reaction (τ_1), i.e. $\tau_0 \simeq 1/\epsilon_0^2 D$, $\tau_0 \geqslant \tau_1$, where ϵ_0 is the light absorption coefficient of the solution illuminated through the measuring electrode.

In order to observe electronically excited states ($A^* \xrightarrow{k_1} A^-$), we also require that the reverse electrode reaction of the resulting particle ($A^- \xrightarrow{k_2} A$) should be slow ($k_2 \ll k_1$).

Solution of the diffusion equation with allowance for the generation and decay of the excited states which can take part in electrode reactions gives the following expression for the total charge collected by the electrode:

$$Q = c\sqrt{\frac{D}{k_1}} \cdot \frac{\sqrt{\frac{\varkappa^2}{Dk}}}{1+\sqrt{\frac{\varkappa^2}{Dk}}} , \qquad (14)$$

where c is the concentration of the particles, D is their diffusion coefficient, k is the unimolecular rate constant for the decay of excited species in solution, and κ is the rate constant of the electrode reaction.

The initial concentration of excited states is determined by the concentration of the initial compound and by the quantum yield of the photochemical reaction (usually $c \simeq 10^{-7}$ M cm^{-3}). It is found that the maximum charge collected by the electrode corresponds to $\kappa \geqslant 10^3$ cm s^{-1} for singlet excited states with $\tau_0 = 10^{-8}$ s, and to $\kappa \geqslant 10^{-1}$ cm s^{-1} for triplet states with $\tau_0 = 10^{-2}$ s. The second-order decay of the states in the bulk of the solution, e.g. by radical dimerisation or disproportionation, gives rise to a non-linear relation between the measured charge and the initial concentration of metastable states.

If the photochemical reaction in solution produces two metastable particles in a single event, the form of the electrode current will depend on the rate of the electrode reaction, the diffusion coefficient, and the direction of electron transfer through the interface for each of the particles.

We have studied[96] the photocurrents produced by illumination of aqueous solutions of riboflavin and sodium salts of the 1-, 2-, and 2,6-sulphonic acids of 9,10-anthraquinone in their absorption band, so that photoemission currents were negligible. The photocurrent pulse consists of two parts: a cathodic current with a rise time of $\leqslant 10^{-4}$ s, followed by an anodic current with a rise time of $\sim 5 \times 10^{-3}$ s. The variation of the initial part of the photocurrent with voltage, concentration, light intensity, and other parameters shows that this current is due to particles generated in the bulk of the solution, reaching the electrode by diffusion, and disappearing mainly in the bulk of the solution. The rate constant for the electrode reduction of this species is fairly large. The species could be an OH radical, formed by the reaction between an excited quinone molecule and a water molecule or a hydroxyl ion. The characteristics of the slow part of the signal indicate that the phenomenon involves oxidation and reduction at the electrode of the riboflavin semiquinones and of the anthraquinone derivatives.

REFERENCES

1. E. Becquerel, Compt. rend., 9, 145 (1839).
2. G. C. Barker and A. W. Gardner, Symposium, "Basic Problems in Modern Theoretical Electrochemistry" (Translated into Russian), Izd. Mir, 1965, p. 148.
3. G. C. Barker, A. W. Gardner, and D. C. Sammon, J. Electrochem. Soc., 113, 1182 (1966).
4. G. C. Barker, Electrochim. Acta, 13, 1221 (1968).
5. Yu. Ya. Gurevich, A. M. Brodskii, and V. G. Levich, Elektrokhimiya, 3, 1302 (1967).
6. A. M. Brodskii and Yu. Ya. Gurevich, Zhur. Eksper. Teor. Fiz., 54, 213 (1968).
7. A. M. Brodskii and Yu. Ya. Gurevich, Izv. Akad. Nauk SSSR, Ser. Fiz., 33, 388 (1969).
8. L. I. Korshunov, Ya. M. Zolotovitskii, and V. A. Benderskii, Elektrokhimiya, 4, 499 (1968).
9. L. I. Korshunov, V. A. Benderskii, V. I. Gol'danskii, and Ya. M. Zolotovitskii, Pis'ma Zhur. Eksper. Teor. Fiz., 7, 55 (1968).
10. L. I. Korshunov, Ya. M. Zolotovitskii, and V. A. Benderskii, Elektrokhimiya, 5, 716 (1969).
11. Yu. V. Pleskov and Z. A. Rotenberg, J. Electroanalyt. Chem., 20, 1 (1969).
12. (no Ref. 12).
13. M. Heyrovsky, Z. Phys. chem., 52, 1 (1967).
14. R. De. Levie and A. A. Husovsky, J. Electroanalyt. Chem., 20, 181 (1969).
15. Z. A. Rotenberg, Yu. Ya. Gurevich, and Yu. V. Pleskov, Elektrokhimiya, 4, 1086 (1968).
16. H. Berg, H. Schweiss, and D. Tresselt, Exptl. Tech. Phys., 12, 116 (1964).
17. V. P. Sharma, P. Delahay, G. G. Susbiels, and G. Tessary, J. Electroanalyt. Chem., 16, 285 (1968).
18. L. I. Korshunov, Ya. M. Zolotovitskii, and V. A. Benderskii, Elektrokhimiya, 7, 477 (1971).
19. P. Delahay and V. S. Srinivasan, J. Phys. Chem., 70, 420 (1966).
20. L. I. Korshunov, Thesis, Chernogolovka, 1970.
21. L. I. Gal'perin, L. B. Mashkinov, V. A. Benderskii, Yu. S. Shcherbinin, and A. G. Lavrushko, Pribory i Tekh. Eksper., No. 1, 288 (1969).
22. L. I. Korshunov, V. P. Tychinskii, et al., Pis'ma Zhur. Eksper. Teor. Fiz. (in the Press).
23. M. Heyrovsky and A. G. Norrish, Nature, 200, 800 (1963).
24. M. Heyrovsky, Nature, 206, 1356 (1965).
25. M. Heyrovsky, Nature, 209, 708 (1966).
26. M. Heyrovsky, Abh. Dtsch. Acad. Wiss., Berlin, Klass. f. Medizin, 4, 409 (1966).
27. M. Heyrovsky, Proc. Roy. Soc. A, 301, 411 (1967).
28. H. Berg, Coll. Czech. Chem. Comm., 25, 3404 (1960).
29. H. Berg, First Jena Symposium 1962, "Polarographie in Chemietherapie, Biochemie, Biologie", Academ. Verlag, Berlin, 1967, p. 128.
30. H. Berg and H. Schweiss, Electrochim. Acta, 9, 425 (1964).
31. H. Berg, Rev. Polarography (Kyoto), 11, 29 (1963).
32. H. Berg, H. Schweiss, E. Stutter, and K. Weller, J. Electroanalyt. Chem., 15, 415 (1967).
33. H. Berg, Electrochim. Acta, 13, 1249 (1968).
34. F. P. Bowden, Trans. Faraday Soc., 27, 505 (1931).
35. A. V. Sokolov, "Opticheskie Svoistva Metallov" (Optical Properties of Metals), Fizmatgiz, Moscow, 1961.
36. R. H. Fowler, Proc. Roy. Soc. A, 118, 229 (1928).

37. R. H. Fowler, Phys. Rev., 38, 45 (1931).
38. R. L. Platzman, "Basic Mechanisms in Radiobiology", Publ. No. 305, U. S. Nat. Res. Council, 1953.
39. Yu. Ya. Gurevich and Z. A. Rotenberg, Elektrokhimiya, 4, 529 (1968).
40. L. E. Price, Thesis, Cambridge, 1938.
41. P. J. Hillson and E. K. Rideal, Proc. Roy. Soc. A, 192, 295 (1949).
42. R. de Levie and J. C. Kreuser, J. Electroanalyt. Chem., 21, 221 (1969).
43. Yu. I. Malov, Thesis, Kiev, 1967.
44. A. N. Frumkin, Elektrokhimiya, 1, 394 (1965).
45. L. I. Korshunov, Ya. M. Zolotovitskii, and V. A. Benderskii, Elektrokhimiya, 7, 75 (1971).
46. L. I. Dobretsov and M. V. Gomoyunova, "Emissionnaya Elektronika" (Emission Electronics), Izd. Nauka, Moscow, 1966, p. 270.
47. G. Brigleb and J. Czenala, Angew. Chem., 72, 401 (1960).
48. L. I. Korshunov, Ya. M. Zolotovitskii, and V. A. Benderskii, Khim. Vysokikh Energyy, 4, 461 (1970).
49. R. Gordon, J. Chem. Phys., 48, 90 (1968).
50. L. P. Beruchashvili, V. I. Shubin, P. I. Dolin, and V. I. Zolotarevskii, Dokl. Akad. Nauk SSSR, 174, 1115 (1967).
51. A. M. Goodman, Phys. Rev., 144, 588 (1966).
52. W. Ludwing and B. Korneffel, Phys. Stat. Sol., 24, K137 (1967).
53. A. J. Braunstein, M. Braunstein, and G. S. Picus, Phys. Rev. Letters, 15, 956 (1965).
54. A. Waxman, J. Appl. Phys., 38, 4763 (1967).
55. A. Braunstein, M. Braunstein, G. C. Picus, and C. A. Mead, Phys. Rev. Letters, 14, 219 (1965).
56. F. L. Schuermaer, C. R. Young, and J. M. Blasingame, J. Appl. Phys., 39, 1791 (1968).
57. V. M. Byakov, L. T. Bugaenko, and B. V. Ershler, Paper to the 20th International Conference on Theoretical and Applied Chemistry, Moscow, 1965.
58. H. A. Schwarz, Proceedings of the Fifth Informal Conference on the Radiation Chemistry of Water, Notre Dame, 1966, p. 51.
59. K. Beckurts and K. Wirtz, "Neitronnaya Fizika" (Neutron Physics), Atomizdat, Moscow, 1968, p. 199.
60. V. M. Agranovich, "Teoriya Eksitonov" (Theory of Excitons), Izd. Nauka, Moscow, 1969.
61. R. K. Wolf, M. J. Bronskill, and J. W. Hunt, J. Chem. Phys., 53, 4201 (1970).
62. J. H. Baxendale and S. Gordon, Symposium on Pulse Radiolysis, Manchester, 1965.
63. D. M. Brown and F. S. Dainton, Symposium "Chemical Kinetics and Chain Reactions" (Translated into Russian), Izd. Nauka, Moscow, 1966, p. 457.
64. Z. A. Rotenberg and Yu. V. Pleskov, Elektrokhimiya, 5, 982 (1969).
65. L. I. Korshunov, Ya. M. Zolotovitskii, and V. A. Benderskii, Elektrokhimiya, 7, 985 (1971).
66. L. I. Korshunov, Ya. M. Zolotovitskii, and V. A. Benderskii, Abstracts of Papers Presented to the All-Union Conference on Electrochemistry, Tbilisi, 1969, p. 343.
67. L. I. Korshunov, Ya. M. Zolotovitskii, V. A. Benderskii, and V. I. Gol'danskii, Khim. Vysokikh Energii, 4, 346 (1970).
68. Ya. M. Zolotovitskii, L. I. Korshunov, and V. A. Benderskii, see Ref. 66, p. 281.
69. Ya. M. Zolotovitskii, L. I. Korshunov, and V. A. Benderskii, Izv. Akad. Nauk SSSR, Ser. Khim., No. 9 (1971).
70. B. B. Damaskin, O. A. Petrii, and V. V. Batrakhov, "Adsorbtsiya Organicheskikh Soedinenii na Elektrodakh" (Adsorption of Organic Compounds on Electrodes), Izd. Nauka, Moscow, 1968.
71. K. Iguchi, J. Chem. Phys., 48, 1735 (1968).
72. K. Fueki, J. Chem. Phys., 49, 765 (1968).
73. J. Appel, "Solid State Physics", Academic Press, New York–London, 1968, Vol. 21, p. 193.
74. Y. Toyozawa, Progr. Theoret. Phys. (Kyoto), 12, 421 (1954).
75. F. V. Bunkin and M. V. Fedorov, Zhur. Eksper. Teor. Fiz., 48, 1341 (1965).
76. D. C. Grahame, J. Amer. Chem. Soc., 79, 2093 (1957).
77. Ya. M. Zolotovitskii, L. I. Korshunov, and V. A. Benderskii, Izv. Akad. Nauk SSSR, Ser. Khim., 1444 (1971).
78. A. B. Karnik and K. M. Joshi, J. Indian Chem. Soc., 42, 127 (1965); 45, 825 (1968).
79. S. P. Perone and J. R. Birc, Analyt. Chem., 38, 1589 (1966).
80. H. Mauser and B. Nicel, Naturwiss., 26, 903 (1967).
81. D. Schulte-Frohlinde and C. Sonntag, Z. phys. Chem., 44, 314 (1965).
82. H. Mauser and V. Sproesser, Chem. Ber., 97, 2260 (1964).
83. H. Mauser and V. Bihl, Electrochim. Acta, 11, 1119 (1966).
84. K. Nakada and M. Sato, J. Electrochem. Soc. Japan, 34, 28 (1966).
85. K. Tokyda and C. Ikarami, J. Chem. Soc. Japan, Indust. Chem. Sect., 72, 105 (1969).
86. N. Kamila and M. Okawara, Denki Kagaku, 36, 506 (1968).
87. R. A. Durst and J. K. Taylor, J. Res. Nat. Bur. Stand., 69A, 517 (1965).
88. G. V. Fomin, L. A. Blyumenfel'd, and B. M. Sukhorukov, Dokl. Akad. Nauk SSSR, 157, 1199 (1964).
89. A. N. Terenin, "Fotonika Molekul Krasitelei i Rodstvennykh Organicheskikh Soedinenii" (Photon Physics of Dye Molecules and Related Organic Compounds), Izd. Nauka, Moscow–Leningrad, 1967.
90. E. Rabinowitch, J. Chem. Phys., 8, 551 (1940).
91. F. Silverman and G. Eisenberg, Electrochim. Acta, 5, 1 (1961).
92. H. Berg, Z. Chem., 2, 237 (1962).
93. R. Brdicka, Coll. Czech. Chem. Comm., 14, 130 (1949).
94. J. R. Mercell and W. J. Nickerson, Biochim. Biophys. Acta, 14, 303 (1954).
95. A. D. Broadbent, Chem. Comm., 8, 382 (1967).
96. L. I. Korshunov, Ya. M. Zolotovitskii, V. A. Benderskii, and L. A. Blyumenfel'd, Dokl. Akad. Nauk SSSR, 179, 1381 (1968).
97. L. I. Korshunov, Ya. M. Zolotovitskii, and V. A. Benderskii, Symposium, "Polyarograficheskoe Opredelenie Kisloroda v Biologicheskikh Ob'ektakh" (Polarographic Determination of Oxygen in Biological Materials), Izd. Naukova Dumka, Kiev, 1968, p. 54.
98. Ya. M. Zolotovitskii, L. I. Korshunov, L. M. Eichis, V. A. Benderskii, and L. A. Blyumenfel'd, Biofizika, 15, 426 (1970).

99. H. Berg and Golmik, Coll. Czech. Chem. Comm., 30, 4192 (1965).
100. E. Shtutter, Elektrokhimiya, 4, 151 (1968).
101. M. E. Peover, Electrochim. Acta, 13, 1083 (1968).
102. D. L. Maricle and A. H. Maurer, Chem. Phys. Letters, 2, 602 (1968).
103. J. Cheng, D. M. Hercules, and D. M. Roe, Electrochim. Acta, 13, 1197 (1968).
104. R. E. Visco and E. A. Chandross, Electrochim. Acta, 13, 1187 (1968).
105. D. L. Maricle, A. Zweig, A. H. Maurer, and J. S. Brinen, Electrochim. Acta, 13, 1209 (1968).
106. C. A. Parcer and G. D. Short, Trans. Faraday Soc., 63, 2618 (1967).
107. J. M. Bader and T. Kuwana, J. Electroanalyt. Chem., 10, 104 (1965).
108. S. W. Feldberg, J. Amer. Chem. Soc., 88, 390 (1968).
109. K. S. V. Santan and A. J. Bard, J. Amer. Chem. Soc., 87, 139 (1965).
110. S. W. Feldberg, J. Phys. Chem., 70, 3928 (1966).

Institute of Chemical
Physics of the USSR
Academy of Sciences,
Moscow